Available online at www.sciencedirect.com
SCIENCE DIRECT®
Journal of Organometallic Chemistry 666 (2003) 87–101
Journal of Organometallic Chemistry
www.elsevier.com/locate/jorganchem

Structurally adaptive multitopic ligands containing tris(pyrazolyl)methane units as supramolecular synthons: manganese carbonyl complexes

Daniel L. Reger *, Radu F. Semeniuc, Mark D. Smith

Department of Chemistry and Biochemistry, University of South Carolina, Columbia, SC 29208, USA

Received 15 August 2002

Dedicated to Professor Jerry Atwood on the occasion of his 60th birthday

Abstract

The compounds {*p*-$C_6H_4[CH_2OCH_2C(pz)_3]_2[Mn(CO)_3]_2$}$(BF_4)_2$ (**1**, pz = pyrazolyl ring), {*p*-$C_6H_4[CH_2OCH_2C(pz)_3]_2$-$[Mn(CO)_3]_2$}$(OTf)_2$ (**2**, $OTf^- = CF_3SO_3^-$), {*m*-$C_6H_4[CH_2OCH_2C(pz)_3]_2[Mn(CO)_3]_2$}$(BF_4)_2$ (**3**) and {*1,2,4,5*-$C_6H_2[CH_2OCH_2C$-$(pz)_3]_4[Mn(CO)_3]_4$}$(BF_4)_4$ (**4**) have been prepared by reaction of the respective ligands with '$Mn(CO)_5^+$', prepared 'in situ' from the reaction of $Mn(CO)_5Br$ and $AgBF_4$ or AgOTf in refluxing acetone. In the structures of all four complexes, the environment around the manganese atom is a slightly distorted octahedron, with the distortion caused by the restricted bite angle of the κ^3-bonded tris(pyrazolyl)methane ligand. The structurally adaptive ligands in all four complexes support extended three-dimensional (3D) supramolecular structures. An important organizational feature for the three BF_4^- complexes is a double π–π and C–H···π interaction involving the pyrazolyl rings. The double π–π/C–H···π interaction is intermolecular in **1** and **3** leading to the formation of chains and sheets. In the case of the tetratopic ligand in complex **4**, the π–π/C–H···π interaction is intramolecular between adjacent (*ortho*) side arms. These supramolecular structures are also supported by weak C–H···F hydrogen bonds. For **3**, classic π–π interactions of the central arene rings are also involved in organizing the 3D network. For **2**, the structure is organized solely by C–H···O hydrogen bonding.

Keywords: Tris(pyrazolyl)methane ligands; Manganese carbonyl complexes; Supramolecular structure

1. Introduction

Investigations into the architecture of supramolecular compounds formed by self-assembly processes have been ongoing in the last two decades [1]. A growing field in this area is the synthesis and characterization of multidimensional architectures based on organometallic building blocks [2]. The key features that determine the overall structures of supramolecular assemblies are the ligand topicity (i.e. the numbers and types of coordinating groups), flexibility or rigidity of the linker groups joining the coordination sites and the stereochemical preferences of the coordinated metal ion [1b,1c,1d,1e,1f,3]. The role of non-covalent interactions is also recognized as providing organization into complex networks. A wide variety of these interactions, mainly involved with the anions [3a,3b,3c,3d,4] and the solvents, [1h,3b,5] were found to have an impact on the solid state organization of several compounds. Important non-covalent interactions are strong [6] and weak [3e,7] hydrogen bonds, π–π stacking, [8] X–H···π interactions (X = O, N, C) [9], and interhalogen interactions [10].

The way in which these organizational features determine supramolecular structures still needs to be clearly elucidated [11]. Our efforts in this area are based on the chemistry of metal complexes of tris(pyrazolyl)methane ligands (Plate 1) [12], a tripodal neutral ligand set isoelectronic to the more heavily studied

* Corresponding author. Tel.: +1-803-777-2587; fax: +1-803-777-9521.
E-mail address: reger@mail.chem.sc.edu (D.L. Reger).

0022-328X/02/$ - see front matter © 2002 Elsevier Science B.V. All rights reserved.
PII: S0022-328X(02)02043-0

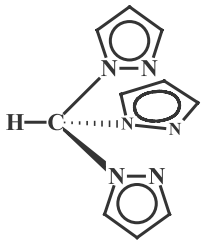

tris(1-pyrazolyl)methane

Plate 1.

tris(pyrazolyl)borate ligands [13]. We have reported substantial improvements in the preparations of tris(pyrazolyl)methane ligands [14] and developed chemistry of them where the central methine carbon atom can be functionalized with groups other than a hydrogen atom [14e].

Using this chemistry, we have prepared multitopic ligands of the general formula C_6H_{6-n}-$[CH_2OCH_2C(pz)_3]_n$, ($n = 2$, 4; pz = pyrazolyl ring). We have reported that the reaction of the three isomers *ortho*-, *meta*- and *para*-$C_6H_4[CH_2OCH_2C(pz)_3]_2$ with $[Cd_2(THF)_5](BF_4)_4$ leads to the formation of coordination polymers of the formula $\{C_6H_4[CH_2OCH_2C(pz)_3]_2$-$Cd(BF_4)_2\}_n$, each with a different supramolecular structure even though they had the same octahedral coordination environment about the cadmium [15]. We have shown that in similar coordination polymers of silver important differences in the coordination mode of the tris(pyrazolyl)methane units as well as on the overall structure were observed [16] Further, the participation of pyrazolyl rings in π–π stacking and C–H···π interactions was observed to be an important organizational feature.

We wished to explore the chemistry of the new multitopic ligands with systems in which the metal was bonded to other ligands that would prevent the formation of coordination polymers. Specifically, we desired a metal system that prefers to bond to the tris(pyrazolyl)methane units in a tripodal fashion and also has nonlabile ligands occupying the remaining coordination sites (these preferences are called the 'reading algorithm' of the metal) [1i,1j]. Given our earlier preparation of $\{$[tris(pyrazolyl)methane]$Mn(CO)_3\}^+$ complexes [14d], we chose $[Mn(CO)_3]^+$ as the metal system. Reported here is the chemistry and description of the solid state structures of $\{p$-$C_6H_4[CH_2OCH_2C(pz)_3]_2[Mn(CO)_3]_2\}$-$(BF_4)_2$ (**1**), $\{p$-$C_6H_4[CH_2OCH_2C(pz)_3]_2[Mn(CO)_3]_2\}$-$(OTf)_2$ (**2**, $OTf^- = CF_3SO_3^-$), $\{m$-$C_6H_4[CH_2OCH_2C$-$(pz)_3]_2[Mn(CO)_3]_2\}(BF_4)_2$ (**3**) and $\{1,2,4,5$-$C_6H_2[CH_2O$-$CH_2C(pz)_3]_4[Mn(CO)_3]_4\}(BF_4)_4$ (**4**). All four complexes have three-dimensional (3D) supramolecular structures in the solid state. We have previously communicated the interesting sinusoidal 3D architecture of **4** [17].

2. Results and discussion

2.1. Synthesis of the compounds

The ligands were prepared as shown in Scheme 1. The compounds $\{p$-$C_6H_4[CH_2OCH_2C(pz)_3]_2[Mn(CO)_3]_2\}$-$(BF_4)_2$ (**1**), $\{p$-$C_6H_4[CH_2OCH_2C(pz)_3]_2[Mn(CO)_3]_2\}$-$(OTf)_2$ (**2**), $\{m$-$C_6H_4[CH_2OCH_2C(pz)_3]_2[Mn(CO)_3]_2\}$-$(BF_4)_2$ (**3**) and $\{1,2,4,5$-$C_6H_2[CH_2OCH_2C(pz)_3]_4[Mn$-$(CO)_3]_4\}(BF_4)_2$ (**4**) were obtained by reaction of the ligands with '$Mn(CO)_5^+$', prepared 'in situ' in refluxing acetone, Scheme 2. Yellow solids were isolated from the reaction mixture. All compounds are stable in air, soluble in acetone, acetonitrile and nitromethane and insoluble in chlorinated solvents or alcohols.

Elemental analysis and electrospay mass spectrometry confirmed the formulated stoichiometry. ESMS spectra showed peaks corresponding to $\{L[Mn(CO)_3]_2BF_4\}^+$ at 954 m/z or $\{L[Mn(CO)_3]_2CF_3SO_3\}^+$ at 1016 m/z and to $\{L[Mn(CO)_3]\}^+$ at 728 m/z for L = bitopic ligands—compounds **1**, **2** and **3**. In the case of **4**, where L is the tetratopic ligand, ESMS experiment revealed peaks at 1919, 1693, 1467 and 1241 m/z corresponding to $\{L[Mn(CO)_3]_4(BF_4)_3\}^+$, $\{L[Mn(CO)_3]_3(BF_4)_2\}^+$, $\{L[Mn(CO)_3]_2(BF_4)\}^+$ and $\{L[Mn(CO)_3]\}^+$, respectively. The double charged species $\{L[Mn(CO)_3]_4(BF_4)_2\}^{++}$ and $\{L[Mn(CO)_3]_2\}^{++}$ were also identified at 916 and 690 m/z, respectively. IR spectra of all the complexes show two bands for the CO ligand in the range 2055–1940 cm^{-1}, suggesting an octahedral coordination around the manganese atoms with three *fac* CO ligands and the $[C(pz)_3]$ units acting as tripodal ligands.

2.2. Solid state structures

Crystals suitable for X-ray diffraction were grown by vapor phase diffusion of diethyl ether into an acetonitrile solution of the compounds. Crystallographic data and structure refinement parameters for compounds **1** and **2** are listed in Table 1 and for **3** and **4** in Table 2. Selected bond lengths and angles are listed in Tables 3 and 4, respectively.

X-Ray analysis revealed that the structure of each binuclear building block of **1** (Fig. 1) has the [tris(pyrazolyl)methane]$Mn(CO)_3$ units located in a *trans* arrangement above and below the plane of the arene ring. The angle formed by the ring and the plane of the attached CH_2OCH_2 group is 87°. The environment around the manganese atom is a slightly distorted octahedron, with the distortion caused by the restricted bite angle of the κ^3-bonded tris(pyrazolyl)methane ligand.

These homobimetallic building blocks are associated into a more complex architecture by simultaneous intermolecular π–π and C–H···π interactions between

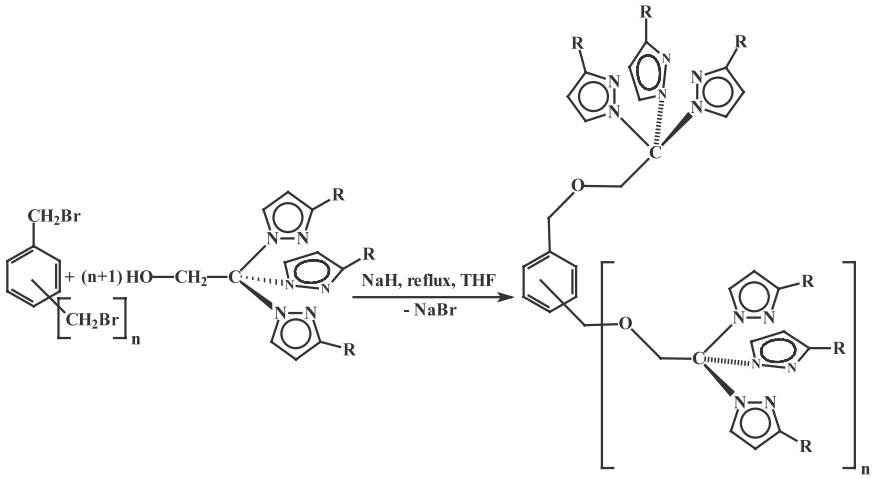

R = H; n = 1: ortho
meta
para
n = 3: 1,2,4,5

Scheme 1.

$$n\ Mn(CO)_5Br + n\ AgX \xrightarrow[-\ n\ AgBr]{\text{acetone, reflux 1h}} n\ ''\ Mn(CO)_5X\ ''$$

$$C_6H_{6-n}[CH_2OCH_2C(pz)_3]_n + n\ ''\ Mn(CO)_5X\ ''$$

$$\downarrow \quad \text{acetone, reflux 2h}; \ -2n\ CO$$

$$\{C_6H_{6-n}[CH_2OCH_2C(pz)_3]_n[Mn(CO)_3]_n\}X_n$$

n = 2, para, $X = BF_4^-$; 1
$X = OTf^-$; 2
meta, $X = BF_4^-$; 3
n = 4, 1,2,4,5, $X = BF_4^-$; 4

Scheme 2.

two tris(pyrazolyl)methane units located in adjacent binuclear building block, as shown in a general representation in Scheme 3.

Arrangement of the $[C(pz)_3]$ units along the C_3 axis in the way depicted aligns two pyrazolyl rings so as to be involved in a π–π interaction, with the nitrogen atoms oriented in opposite directions so as to maximize the attraction [8]. This orientation directs the hydrogen atoms located at the 4-position of each pyrazolyl ring involved in the π–π interaction toward to a second pyrazolyl ring, forming a C–H···π interaction. The intrinsic geometry of the tris(pyrazolyl)methane units makes this double interaction a highly favored arrangement for the non-covalent forces.

The pyrazolyl rings in each tris(pyrazolyl)methane unit of **1** form these types of π–π/C–H···π interactions with both neighboring units as pictured in Fig. 2a. The pyrazolyl ring centroid–centroid distance, 3.61 Å, is well below the maximum accepted distance (3.8 Å) for π–π interaction [8]. The third pyrazolyl ring that is not involved in π–π stacking interactions acts as an acceptor for both C–H donor groups from the two pyrazolyl rings involved in the π–π stacking. The C–H–centroid distances of the associated C–H···π interactions are 2.73 and 2.94 Å and the corresponding C–H–centroid angles are 145.1 and 133.8°. These values are typical for C–H···π interactions [9]. These non-covalent forces organize the bimetallic building blocks into stair-shaped 2D sheets, Fig. 2b.

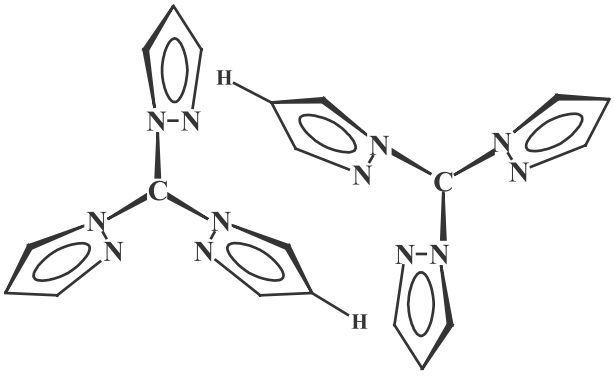

Scheme 3.

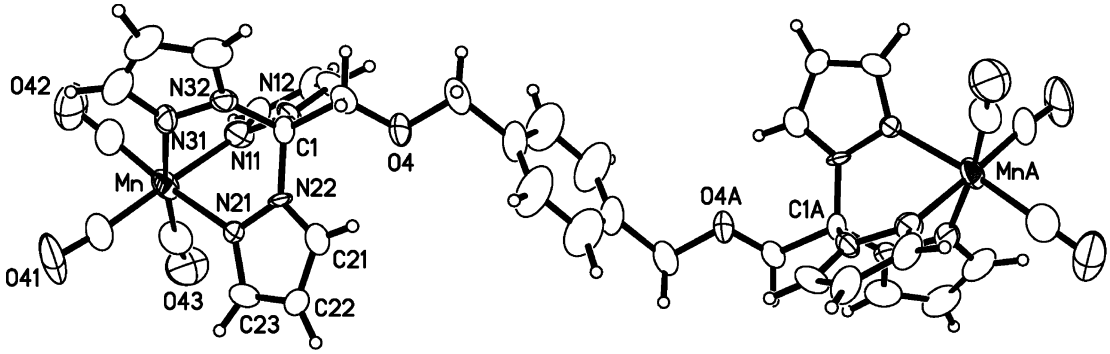

Fig. 1. ORTEP representation and numbering scheme of cationic part of $\{p\text{-}C_6H_4[CH_2OCH_2C(pz)_3]_2[Mn(CO)_3]_2\}(BF_4)_2$ (**1**).

Fig. 3a shows of how the sheets, oriented as in Fig. 2b, are joined in a 3D network by the BF_4^- groups through weak C–H···F hydrogen bonds. One fluorine atom makes a bifurcated hydrogen bond with two separate building blocks with the rest of the fluorine atoms being involved each in only one hydrogen bond with two additional building blocks. Fig. 3b shows the interactions of one BF_4^- group bridging two of the sheets. It also bridges two pairs of tris(pyrazolyl)methane units within the sheets that are also involved in π–π interactions, strengthening the forces that join the units into 2D sheets. The distances and angles of these interactions are shown in Table 5. The average of the (C)H···F values in Table 5 is nearly 0.2 Å shorter than the sum of the van der Waals radii for H and F atoms, 2.54 Å [18].

Fig. 4 is a view along the 11 × 8 Å channels formed by the self-organization of $\{p\text{-}C_6H_4[CH_2OCH_2C(pz)_3]_2\text{-}[Mn(CO)_3]_2\}(BF_4)_2$ into a 3D architecture. The channels run at an oblique angle to the [010] direction in the unit cell. The channels are filled with the guest solvent molecules acetone and ether, occupying 1222 $Å^3$ from the total of 3073 $Å^3$ of the unit cell.

The complex $\{p\text{-}C_6H_4[CH_2OCH_2C(pz)_3]_2[Mn(CO)_3]_2\}(OTf)_2$ (**2**), that contains the same binuclear building block as **1** but a different counter-ion, has a different structure, a structure that is also built by non-covalent interactions. X-ray analysis of **2** revealed the same octahedral arrangement of the $[C(pz)_3][Mn(CO)_3]$ units, Fig. 5. However, the side arms of the linking ether groups are in a skewed position with respect to the arene plane. The angle formed by the ring and the plane of the attached CH_2OCH_2 group is 64° with the unusual feature that both ether linkages are skewed in the same direction (see also Fig. 6b), the first time we have observed this type of arrangement [15,16]. In

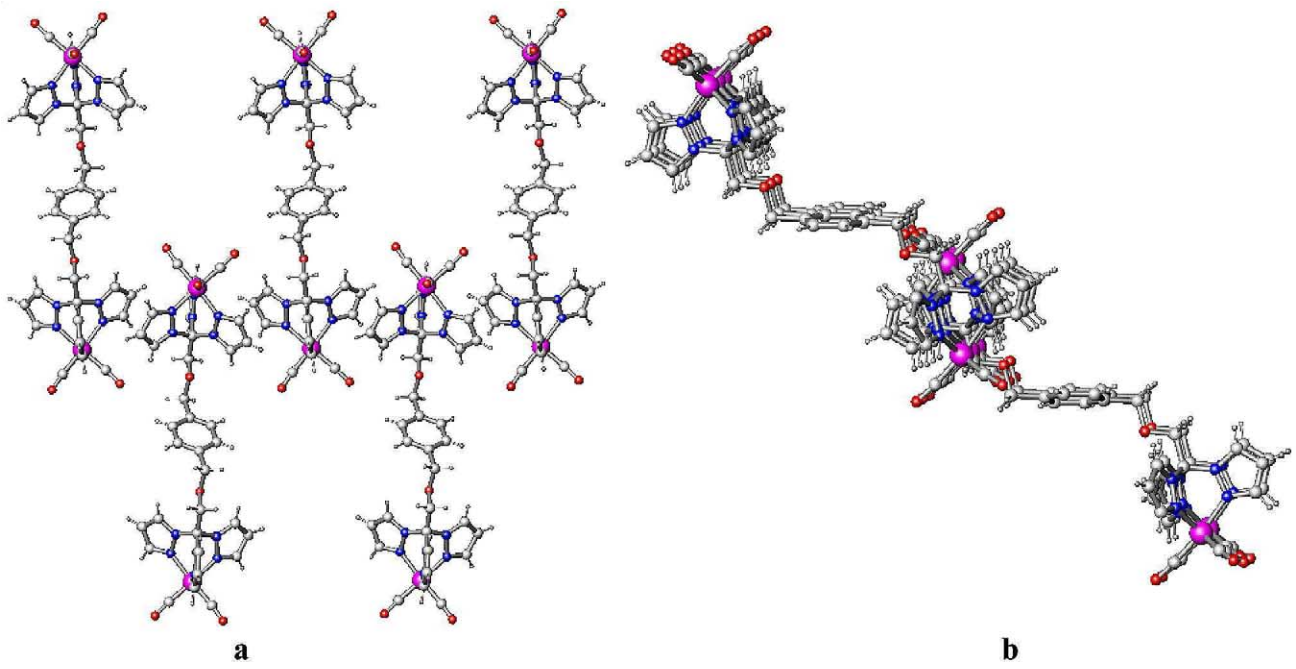

Fig. 2. The 2D sheet for **1** formed by intermolecular π–π/C–H···π interactions: (a) view perpendicular on sheet; (b) view parallel to sheet, showing the stair-like arrangement of the sheet.

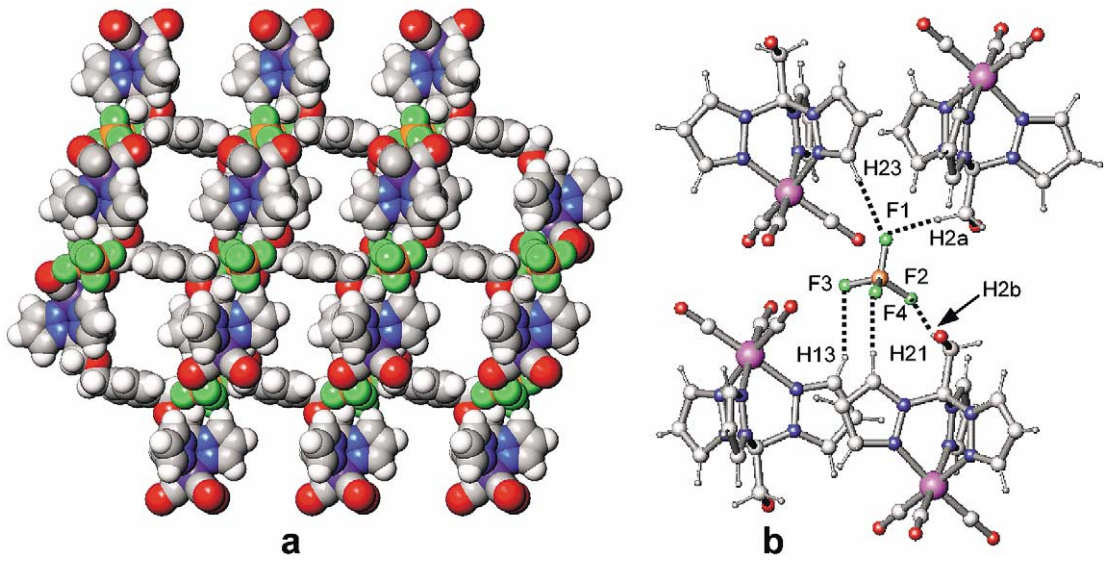

Fig. 3. (a) Space filling representation of the 3D network for **1** formed via week C–H···F hydrogen bonds; (b) C–H···F intermolecular interactions for one BF_4^- bridging two pairs of tris(pyrazolyl)methane units (also involved in π–π interactions) in each sheet and also bridging two of the sheets.

contrast to **1**, there are no π–π stacking or C–H···π interactions between the $[C(pz)_3]$ units. Since all other conditions in the preparation and crystallization of **2** were identical as for **1** (method of crystallization, solvents, temperature), the exchange of BF_4^- for $CF_3SO_3^-$ anions dramatically alters the non-covalent interactions. Because the oxygen atoms from the $CF_3SO_3^-$ anion can form stronger hydrogen bonds than fluorine atoms from the BF_4^- anion, the dominate non-covalent force in **2** is C–H···O hydrogen bonding [19]. Unfortunately, the triflate anions were found to be disordered and a precise assessment of these interactions cannot be made. However, the three views of the overall structure shown in Fig. 6, each oriented 90° with respect to one another, indicate an interesting supramolecular structure organized by the triflate anions. A similar domination of the non-covalent forces by the triflate anion has been observed in the structure of $[\{p\text{-}C_6H_4[CH_2OCH_2C(pz)_3]_2Ag_2\}(OTf)_2]_n$ [20].

Single crystal X-ray analysis of $\{m\text{-}C_6H_4[CH_2O\text{-}CH_2C(pz)_3]_2[Mn(CO)_3]_2\}(BF_4)_2$ (**3**), the *meta* isomer of **1**, revealed that the binuclear organometallic building block has both $[C(pz)_3][Mn(CO)_3]$ units on the same side of the central arene ring, Fig. 7. Again, the environment around the manganese atom is a slightly distorted octahedron, with the distortion caused by the restricted bite angle of the κ^3-bonded tris(pyrazolyl)methane ligand. Details on the geometric parameters of the cationic unit can be found in Table 4.

The supramolecular structure of **3** is based almost entirely on π–π stacking and C–H···π interactions. First, two pairs of pyrazolyl rings are involved in two separate interactions, connecting the building blocks head to tail into corrugated chains. The corresponding values for the interactions are as follows: for the first pair of pz rings the centroid–centroid distance is of 3.38 Å and the H(12)–centroid distance is 2.90 Å, with a C–H–centroid angle of 143.5°. For the second pair the same distances are 3.66, 2.86 Å and 140.9°, respectively. Fig. 8a is a view perpendicular to one corrugated chain, showing the π–π stacking component of one double π–π/C–H···π interaction. The chains run along the body diagonal of the unit cell (crystallographic [111] direction), as can be seen in Fig. 8b. A third pair of pyrazolyl rings is involved in another π–π/C–H···π interaction, with the corresponding geometric parameters of 3.72, 2.96 Å and 137.6°. This last interaction organizes the

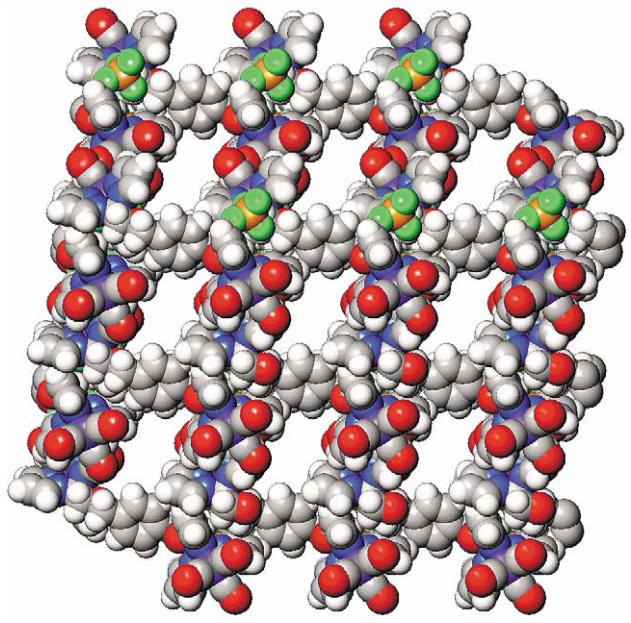

Fig. 4. View for **1** along the channels formed by the 3D architecture; solvent molecules are not shown.

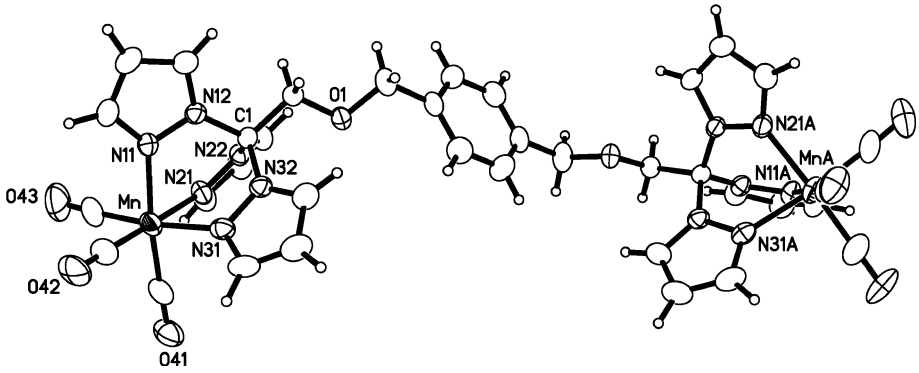

Fig. 5. ORTEP representation and numbering scheme of cationic part of $\{p\text{-}C_6H_4[CH_2OCH_2C(pz)_3]_2[Mn(CO)_3]_2\}(OTf)_2$ (**2**).

chains into a 2D sheet of chains. Two chains showing one connection between the chains are pictured in Fig. 9a, with Fig. 9b being a view end-on to that of Fig. 9a.

An interesting structural feature of **3** is that the central arene ring is involved in a classic π–π interaction organizing the 2D sheets into a 3D network. The placement of both side arms of any bimetallic building block on the same side of the central arene ring allows an arrangement where two arene rings from different sheets are situated one above another and parallel displaced, orienting the side arms in opposite directions, Fig. 10a. This offset leads to a long centroid–centroid distance (4.13 Å) but with a short perpendicular distance between the planes of 3.64 Å. Fig. 10b shows that the BF_4^- anions are also involved in the organization of **3** into a 3D architecture. Each BF_4^- makes two hydrogen bonds (the values are listed in Table 5), one with a building block within one sheet and another one with a building block next to the one involved in the 'classic' π–π stacking from a neighboring sheet, contributing in this manner to the strength that organize the sheets into a 3D structure, Fig. 11.

Crystals of the manganese complex of the tetratopic ligand have the formula $\{C_6H_2[CH_2OCH_2C(pz)_3]_4[Mn(CO)_3]_4\}(BF_4)_4\cdot 6CH_3CN\cdot 2C_4H_{10}O$ (**4**). Single crystal X-ray analysis shows that as in the other cases, each of the tris(pyrazolyl)methane units of the ligand is κ^3-bonded to a $[Mn(CO)_3]^+$ cation forming a distorted octahedral arrangement around the manganese(I), Fig. 12. The overall structure of the centrosymmetric tetrametallic building block is surprising in that the *ortho*-bonded ligand side arms are on the same side of the connecting arene ring. In the structures of *o*-$C_6H_4[CH_2OCH_2C(pz)_3]_2$ and 1,2,4,5-$C_6H_2[CH_2O$-

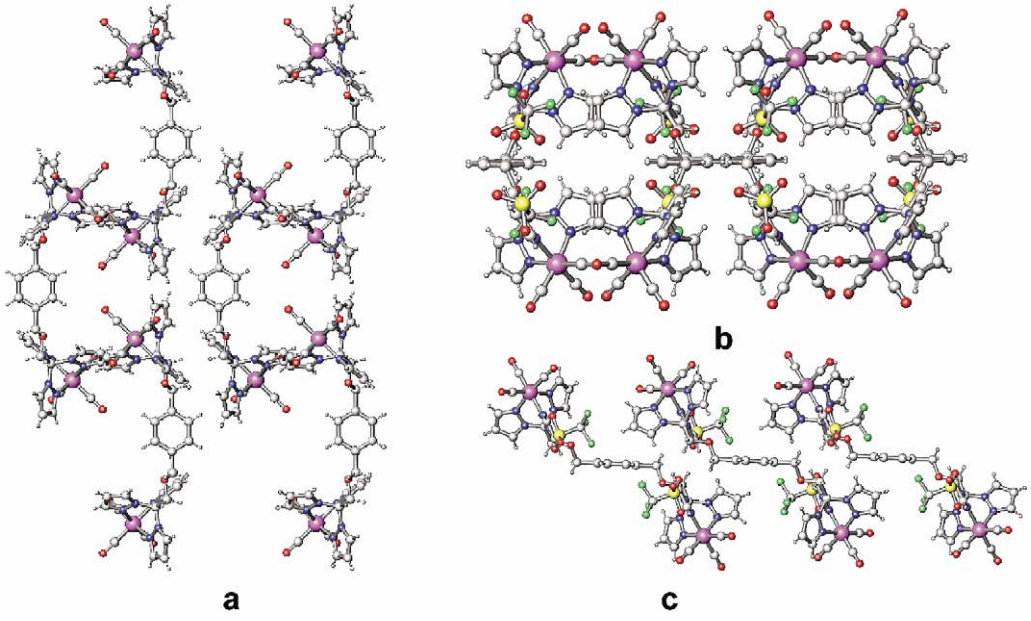

Fig. 6. Extended structures of **2**: (a) six cationic binuclear building blocks aligned perpendicular to *b* axis of the unit cell; triflate anions not shown; (b) the same six building blocks viewed down *c* axis showing the skewed *trans* position with respect to the central arene plane and the position of the triflate anions; (c) view down *b* axis showing the stair-like shape of the building blocks.

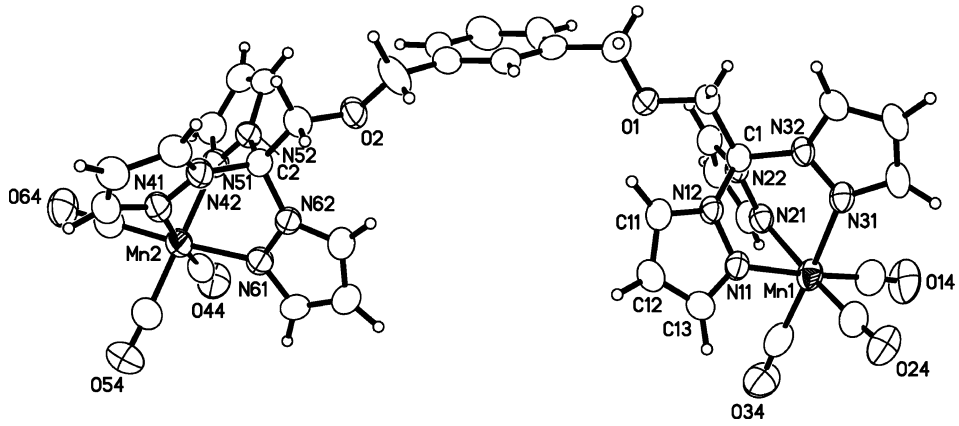

Fig. 7. ORTEP representation and numbering scheme of cationic part of $\{m\text{-}C_6H_4[CH_2OCH_2C(pz)_3]_2[Mn(CO)_3]_2\}(BF_4)_2$ (**3**).

$CH_2C(pz)_3]_4$ and the coordination polymers $\{o\text{-}C_6H_4[CH_2OCH_2C(pz)_3]_2Cd(BF_4)_2\}_n$ and $\{1,2,4,5\text{-}C_6H_2[(CH_2OCH_2C(pz)_3]_4Ag_2(BF_4)_2\}_n$, adjacent side-arms are on opposite sides of the central arene ring [15,16a]. The driving force for the same side organization observed here is an intramolecular π–π/C–H···π interaction, between two pyrazolyl rings located on adjacent arms. The perpendicular distance between the pyrazolyl rings planes is 3.50 Å and the centroid–centroid distance is 3.53 Å. The corresponding C–H···π geometric parameters are 2.66 Å for the H–centroid distance with a C–H–centroid angle of 141.3° for the first pair of side arms and 2.63 Å and 140.9°, respectively, for the second pair. The pairs of adjacent arms are on opposite sides of the arene ring yielding an overall stepped structure for each tetrametallic building block.

As shown in Fig. 13, the tetrametallic building blocks are organized into a 3D architecture by weak C–H···F hydrogen bonds. The supramolecular structure of **1** is a sinusoidal like 'function' with respect to the *b* axis; the 'wave length'—measured between three consecutive phenyl centroids from the same sheet—is equal to the *b* axis, 17.6246(13) Å. There are two BF_4^- anions per asymmetric unit; both are involved in weak hydrogen bonds with different organizational functions. One is involved in organizing the tetrametallic building blocks into 2D corrugated sheets and the second organizes the sheets into a 3D network.

3. Conclusion

We have prepared and characterized in the solid state four complexes containing octahedral $[C(pz)_3][Mn-$

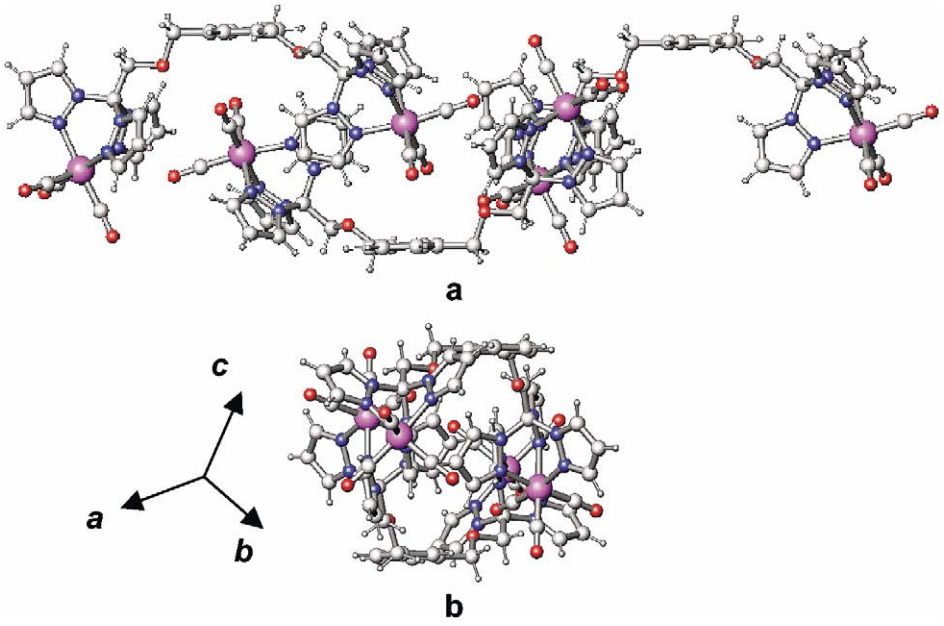

Fig. 8. One corrugated chain constructed by **3**: (a) view perpendicular to the chain; (b) view along the chain.

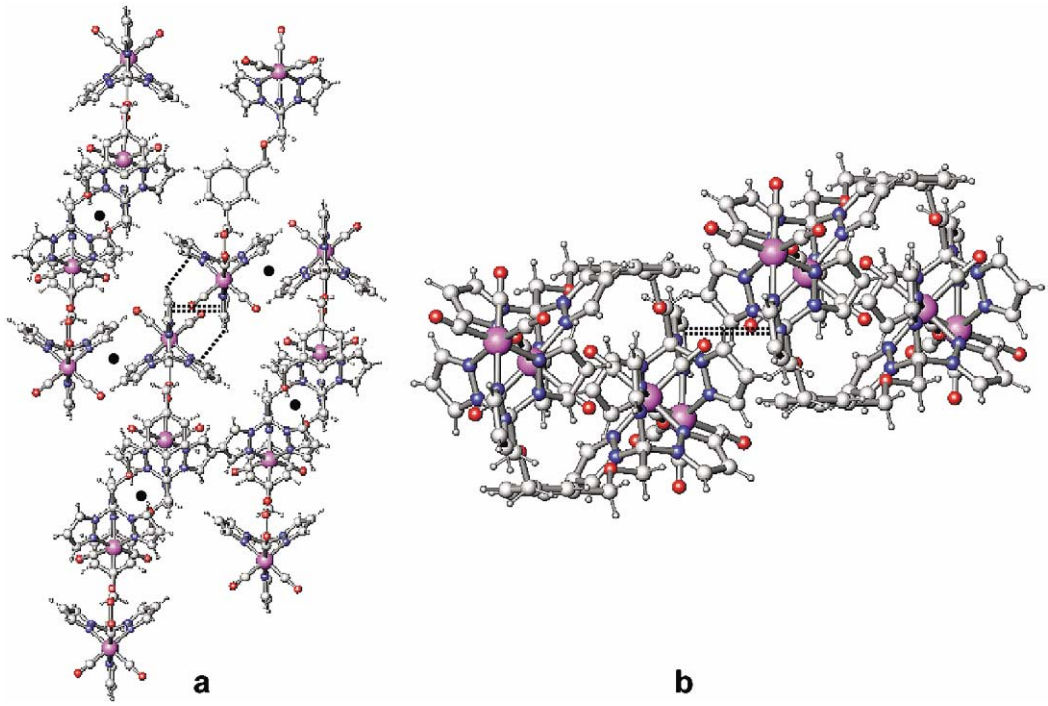

Fig. 9. The association of two chains for **3** into a 2D network: (a) the double π–π/C–H···π interaction that organize the chains into sheets, represented by double dotted/single dotted lines. The dots (●) shows where the double π–π/C–H···π interaction forms the chains presented in Fig. 8; (b) view perpendicular to the two connected chains in the same orientation as in Fig. 8b.

$(CO)_3$] units linked by organic spacers into multinuclear organometallic building blocks. All four organometallic building blocks are organized into complex supramolecular architectures by non-covalent forces. Three of the structures, those with BF_4^- counter-ions, display an interesting π–π stacking in which the pyrazolyl rings involved in the stacking are also associated with a C–H···π interaction. This double π–π/C–H···π interaction is an intrinsic feature of adjacent tripodal tris(pyrazolyl)methane units oriented along the C_3 axis.

There are several conditions that must be fulfilled to observe this interaction. First, the metallic center must

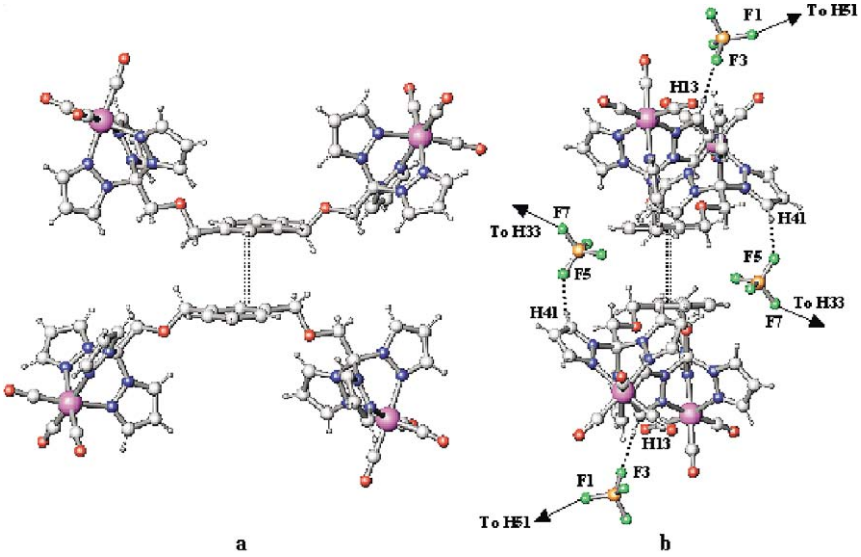

Fig. 10. Organization of **3** into a 3D architecture: (a) classic π–π stacking between two cationic building blocks represented by the double dotted line; (b) the same two building blocks viewed after a 90° rotation; the dotted lines represent weak C–H···F hydrogen bonds between four BF_4^- units and the cationic building blocks involved in the classic π–π stacking; the arrows indicate the direction of the second C–H···F hydrogen bond directed toward other units (not shown) that are part from different sheets; the orientation of the building blocks is the same as in Fig. 8b and Fig. 9b.

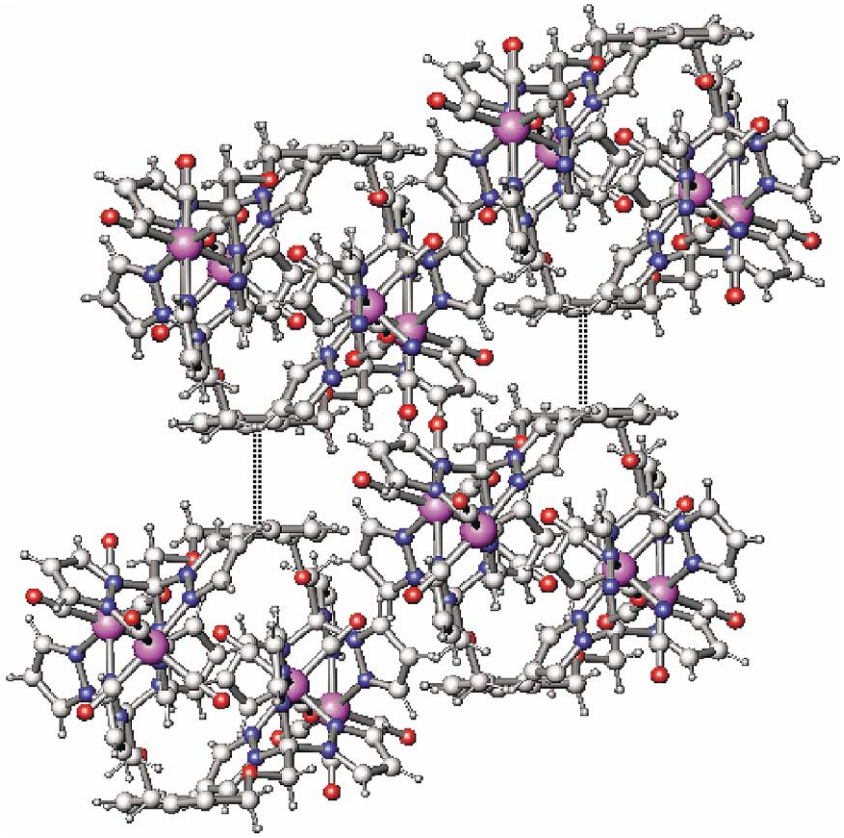

Fig. 11. The overall supramolecular structure of **3** viewed along the body diagonal of the unit cell; for the sake of clarity anions are not shown.

have three open coordination sites so that the $[C(pz)_3]$ unit can act as a tripodal ligand. In previously reported silver coordination polymers based on these same ligands [16a,16b,16c], a κ^2–κ^1 coordination mode of the tris(pyrazolyl)methane unit was observed preventing such a double interaction. Other arrangements of π–π stacking or C–H···π interactions were found to be important organizational tools in those systems, but not the double arrangement observed here for complexes **1**, **3** and **4**. The formation of individual multimetallic

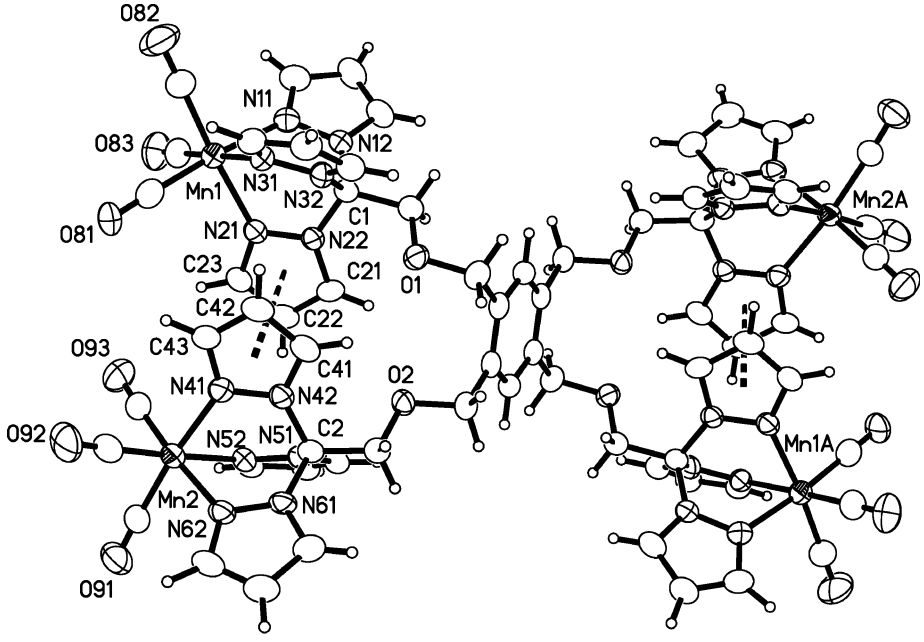

Fig. 12. ORTEP representation and numbering scheme of cationic part of $\{1,2,4,5\text{-}C_6H_2[CH_2OCH_2C(pz)_3]_4[Mn(CO)_3]_4\}(BF_4)_2$ (**4**).

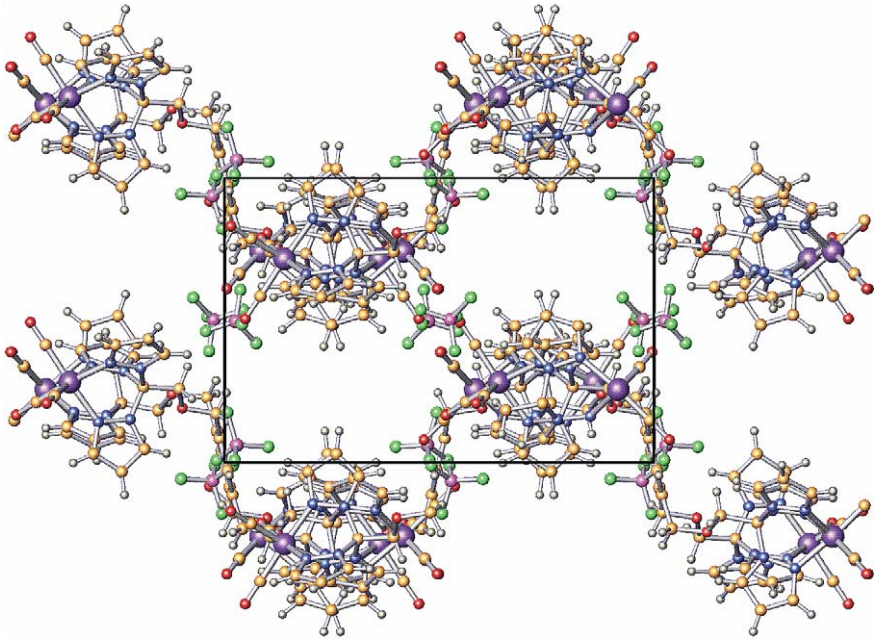

Fig. 13. The supramolecular structure of **4** along the *b* axis.

building blocks, rather than coordination polymers, is also important. In the cadmium coordination polymers of these ligands this double interaction is absent, in spite of the fact that the ligands act as tripodal ligands [15]. The counter-ion is also an important factor for the formation of this double π–π/C–H···π interaction. As we show here, the presence of the triflate anion appears to prevent the double association of the building blocks, presumably due to their greater capacity of establishing weak hydrogen bonds.

The orientation of the [C(pz)$_3$] units within the individual ligands, i.e. ligand topology, also has an

Table 1
Crystallographic data and structure refinement parameters for {*p*-$C_6H_4[CH_2OCH_2C(pz)_3]_2[Mn(CO)_3]_2\}(BF_4)_2$ (**1**) and {*p*-$C_6H_4[CH_2OCH_2C(pz)_3]_2[Mn(CO)_3]_2\}(OTf)_2$ (**2**)

	1	**2**
Empirical formula	$C_{36}H_{30}B_2F_8Mn_2N_{12}O_8$	$C_{42}H_{40}F_6Mn_2N_{12}O_{15}S_2$
Formula weight	1042.22	1240.86
Temperature (K)	173(2)	293(2)
Crystal system	Monoclinic	Monoclinic
Space group	$P2_1/c$	$C2/c$
a (Å)	11.797(3)	22.9560(13)
b (Å)	13.229(3)	12.8233(7)
c (Å)	20.322(5)	20.0778(11)
β (°)	104.299(4)	116.1960(10)
Volume (Å^3)	3073.4(12)	6945.0(9)
Z	2	4
Density (calc.) (Mg m^{-3})	1.126	1.554
Absorption coefficient (mm^{-1})	0.481	0.652
F(000)	1052	2528
Crystal size (mm)	0.46 × 0.20 × 0.10	0.48 × 0.28 × 0.08
Reflections collected	11 441	24 054
Independent reflections	4272 [$R_{int} = 0.0861$]	5420 [$R_{int} = 0.0555$]
Data/restraints/parameters	4272/0/307	5420/43/418
Goodness-of-fit on F^2	0.941	0.975
Final R indices [$I > 2\sigma(I)$]	$R_1 = 0.0953$, $wR_2 = 0.2518$	$R_1 = 0.0572$, $wR_2 = 0.1417$
R indices (all data)	$R_1 = 0.1379$, $wR_2 = 0.2720$	$R_1 = 0.0847$, $wR_2 = 0.1548$

Table 2
Crystallographic data and structure refinement parameters for {*m*-$C_6H_4[CH_2OCH_2C(pz)_3]_2[Mn(CO)_3]_2\}(BF_4)_2$ (**3**) and {1,2,4,5-$C_6H_2[CH_2OCH_2C(pz)_3]_4[Mn(CO)_3]_4\}(BF_4)_2$ (**4**)

	3	**4**
Empirical formula	$C_{36}H_{30}B_2F_8Mn_2N_{12}O_8$	$C_{86}H_{92}B_4F_{16}Mn_4N_{30}O_{18}$
Formula weight	1042.22	2400.90
Temperature (K)	190(2)	173(2)
Crystal system	Triclinic	Monoclinic
Space group	$P\bar{1}$	$P2_1/c$
a (Å)	11.7634(8)	11.8441(9)
b (Å)	12.4354(8)	17.6246(13)
c (Å)	15.8356(11)	25.6874(19)
α (°)	100.856(2)	90
β (°)	99.313(2)	99.538(2)
γ (°)	103.9400(10)	90
Volume (Å^3)	2155.2(3)	5288.1(7)
Z	2	2
Density (calc.) (Mg m^{-3})	1.606	1.508
Absorption coefficient (mm^{-1})	0.686	0.573
F(000)	1052	2452
Crystal size (mm)	0.32 × 0.20 × 0.08	0.40 × 0.24 × 0.20
Reflections collected	16 763	34 997
Independent reflections	6968 [$R_{int} = 0.0531$]	10 830 [$R_{int} = 0.0395$]
Data/restraints/parameters	6968/0/613	10 830/6/712
Goodness-of-fit on F^2	1.011	1.042
Final *R* indices [$I > 2\sigma(I)$]	$R_1 = 0.0601$, $wR_2 = 0.1216$	$R_1 = 0.0688$, $wR_2 = 0.2000$
R indices (all data)	$R_1 = 0.0961$, $wR_2 = 0.1319$	$R_1 = 0.0938$, $wR_2 = 0.2164$

important impact on the overall supramolecular structure. In two cases, the double π–π/C–H···π interaction is intermolecular and leads to the formation of chains and sheets. In these two cases, the shape of the sheets (stair-like or corrugated) is determined by the position of the side arms on the central arene ring. In the case of the tetratopic ligand, the π–π/C–H···π interaction is intramolecular between adjacent (*ortho*) side arms with the counter-ions organizing the building blocks into a 3D network. Our results show that this new class of multitopic ligands, based on tris(pyrazolyl)methane units linked by flexible organic spacers, are structurally adaptive showing a variety of shapes that can accommodate various reading algorithms of different metal systems and maximize non-covalent forces. This structurally adaptive feature of the ligands makes them versatile synthons in supramolecular chemistry.

Table 3
Selected bonds (Å) and angles (°) for **1** and **2**

Atoms	**1**	**2**
Bond lengths		
Mn–N(11)	1.997(6)	2.043(3)
Mn–N(21)	2.044(5)	2.033(3)
Mn–N(31)	2.042(6)	2.045(3)
Mn–C(41)	1.771(9)	1.810(4)
Mn–C(42)	1.782(11)	1.821(4)
Mn–C(43)	1.806(9)	1.810(5)
Bond angles		
N(11)–Mn–N(21)	83.7(2)	85.02(10)
N(11)–Mn–N(31)	83.2(2)	83.23(10)
N(21)–Mn–N(31)	83.8(2)	83.99(10)
C(41)–Mn–C(42)	88.4(4)	90.91(17)
C(41)–Mn–C(43)	89.6(4)	92.57(19)
C(42)–Mn–C(43)	93.9(4)	91.3(2)
C(41)–Mn–N(11)	178.0(3)	174.14(13)
C(42)–Mn–N(11)	93.6(4)	92.81(15)
C(43)–Mn–N(11)	90.6(3)	91.86(16)
C(41)–Mn–N(21)	94.3(3)	91.09(14)
C(42)–Mn–N(21)	173.9(3)	176.94(16)
C(43)–Mn–N(21)	91.6(3)	90.89(16)
C(41)–Mn–N(31)	96.4(4)	92.02(15)
C(42)–Mn–N(31)	90.5(3)	93.63(16)
C(43)–Mn–N(31)	172.6(3)	173.18(15)

4. Experimental

4.1. General procedure

All operations were carried out under a nitrogen atmosphere using standard Schlenk techniques and a Vacuum Atmospheres HE-493 dry box. All solvents were dried, degassed, and distilled prior to use. The ^{1}H-NMR spectra were recorded on a Varian AM300 spectrometer using a broad-band probe. Proton chemical shifts are reported in ppm versus internal Me_4Si. Mass spectral data were recorded on a MicroMass QTOF spectrometer. Clusters assigned to specific ions show appropriate isotopic patterns as calculated for the atoms present. The bitopic ligands were prepared

Table 4
Selected bonds (Å) and angles (°) for **3** and **4**

3		**4**	
Bond lengths			
Mn(1)–N(11)	2.045(4)	Mn(1)–N(11)	2.051(3)
Mn(1)–N(21)	2.052(4)	Mn(1)–N(21)	2.039(3)
Mn(1)–N(31)	2.050(4)	Mn(1)–N(31)	2.035(3)
Mn(1)–C(14)	1.817(6)	Mn(1)–C(81)	1.818(5)
Mn(1)–C(24)	1.798(6)	Mn(1)–C(82)	1.832(4)
Mn(1)–C(34)	1.808(6)	Mn(1)–C(83)	1.809(5)
Mn(2)–N(41)	2.029(4)	Mn(2)–N(41)	2.043(3)
Mn(2)–N(51)	2.044(4)	Mn(2)–N(52)	2.033(3)
Mn(2)–N(61)	2.037(4)	Mn(2)–N(62)	2.046(3)
Mn(2)–C(44)	1.798(6)	Mn(2)–C(91)	1.837(4)
Mn(2)–C(54)	1.817(6)	Mn(2)–C(92)	1.827(5)
Mn(2)–C(64)	1.770(6)	Mn(2)–C(93)	1.810(5)
Bond angles			
N(11)–Mn(1)–N(21)	82.39(14)	N(11)–Mn(1)–N(21)	83.46(12)
N(11)–Mn(1)–N(31)	85.02(14)	N(11)–Mn(1)–N(31)	83.56(13)
N(31)–Mn(1)–N(21)	84.15(14)	N(21)–Mn(1)–N(31)	84.15(12)
C(24)–Mn(1)–C(14)	91.1(2)	C(81)–Mn(1)–C(82)	90.1(2)
C(34)–Mn(1)–C(14)	90.1(2)	C(81)–Mn(1)–C(83)	90.5(2)
C(24)–Mn(1)–C(34)	92.0(2)	C(82)–Mn(1)–C(83)	91.1(2)
C(14)–Mn(1)–N(11)	176.0(2)	C(81)–Mn(1)–N(11)	175.12(16)
C(24)–Mn(1)–N(11)	92.38(18)	C(82)–Mn(1)–N(11)	93.80(18)
C(34)–Mn(1)–N(11)	91.8(2)	C(83)–Mn(1)–N(11)	92.28(17)
C(14)–Mn(1)–N(21)	93.9(2)	C(81)–Mn(1)–N(21)	92.37(15)
C(24)–Mn(1)–N(21)	171.61(18)	C(82)–Mn(1)–N(21)	174.46(17)
C(34)–Mn(1)–N(21)	94.70(19)	C(83)–Mn(1)–N(21)	93.80(16)
C(14)–Mn(1)–N(31)	93.1(2)	C(81)–Mn(1)–N(31)	93.53(16)
C(24)–Mn(1)–N(31)	88.88(19)	C(82)–Mn(1)–N(31)	90.78(17)
C(34)–Mn(1)–N(31)	176.69(19)	C(83)–Mn(1)–N(31)	175.54(17)
N(41)–Mn(2)–N(51)	83.30(16)	N(41)–Mn(2)–N(52)	84.09(12)
N(41)–Mn(2)–N(61)	84.77(15)	N(41)–Mn(2)–N(62)	83.40(12)
N(61)–Mn(2)–N(51)	83.75(15)	N(52)–Mn(2)–N(62)	83.78(12)
C(64)–Mn(2)–C(44)	92.8(2)	C(91)–Mn(2)–C(92)	90.82(19)
C(64)–Mn(2)–C(54)	88.5(2)	C(91)–Mn(2)–C(93)	91.4(2)
C(44)–Mn(2)–C(54)	93.5(2)	C(92)–Mn(2)–C(93)	90.1(2)
C(44)–Mn(2)–N(41)	175.2(2)	C(91)–Mn(2)–N(41)	173.78(16)
C(54)–Mn(2)–N(41)	90.9(2)	C(91)–Mn(2)–N(52)	93.11(16)
C(64)–Mn(2)–N(41)	89.2(2)	C(91)–Mn(2)–N(62)	90.79(17)
C(44)–Mn(2)–N(61)	93.11(19)	C(92)–Mn(2)–N(41)	91.90(16)
C(54)–Mn(2)–N(61)	93.5(2)	C(92)–Mn(2)–N(52)	175.95(16)
C(64)–Mn(2)–N(61)	173.65(19)	C(92)–Mn(2)–N(62)	95.20(19)
C(44)–Mn(2)–N(51)	92.2(2)	C(93)–Mn(2)–N(41)	94.19(16)
C(54)–Mn(2)–N(51)	173.8(2)	C(93)–Mn(2)–N(52)	90.81(17)
C(64)–Mn(2)–N(51)	93.6(2)	C(93)–Mn(2)–N(62)	174.26(17)

following literature methods [15]. 1,2,4,5-$(BrCH_2)_2C_6H_2$, $AgBF_4$, $AgCF_3SO_3$ and $Mn(CO)_5Br$ were purchased from Sigma–Aldrich and used without further purifications.

4.2. Synthesis of 1,2,4,5-$C_6H_2[(CH_2OCH_2C(pz)_3]_4$

To a stirred suspension of NaH (1.2 g, 50 mmol) in THF (250 ml) was added dropwise a mixture of 1,2,4,5-$(CH_2Br)_4C_6H_2$ (1.8 g, 4.0 mmol) and HO–$CH_2C(pz)_3$ (3.9 g, 16 mmol) in THF (100 ml). The solution was heated at reflux for 5 h. Longer reaction times resulted in a darkening of the solution and a subsequent lower yield of the final product. The solution was allowed to cool to room temperature and water (150 ml) was added to consume the excess of NaH and dissolve the salts formed in the reaction. The organic layer was separated, the aqueous layer extracted with ether (3 × 100 ml) and the combined organic extracts were washed with a saturated $NaHCO_3$ solution (200 ml) and with water (200 ml). The organic phase was dried (Na_2SO_4), filtered and the solvent removed in vacuo yielding an off white solid (3.34 g, 76%). ES^+MS: for $[C_{54}H_{54}N_{24}O_4Na]^+$ Calc.: 1125.4658. Found: 1125.4657; ^{1}H-NMR (acetone-d_6 300 Hz): δ 7.61, 7.46 (d of d, 12,12H, 3,5-H pz), 7.04 (s, 2H, C_6H_2), 6.34 (d of d, 12H, 4-H pz), 5.08 (s, 8H, OCH_2pz), 4.46 (s, 8H, $OCH_2C(Ph)_3$).

Table 5
Hydrogen bonding parameters for compounds **1**, **2**, **3** and **4**

Atoms	C···A	H···A	C–H···A
*Compound **1***			
C(13)–H(13)–F(3)	3.33	2.45	154.8
C(21)–H(21)–F(4)	3.21	2.31	156.6
C(2)–H(2B)–F(2)	3.33	2.36	165.5
C(22)–H(23)–F(1)	3.21	2.27	169.3
C(2)–H(2A)–F(1)	3.26	2.34	153.5
*Compound **2***			
C(2)–H(2A)–O(52)	3.24	2.39	145.9
C(2)–H(2A)–O(52)	3.28	2.35	161.6
*Compound **3***			
C(13)–H(13)–F(3)	3.29	2.38	158.3
C(51)–H(51)–F(1)	3.05	2.32	132.5
C(33)–H(33)–F(7)	3.20	2.34	150.1
C(41)–H(41)–F(5)	3.35	2.41	169.5
*Compound **4***			
C(11)–H(11)–F(3)	3.23	2.40	146.0
C(13)–H(13)–F(4)	3.27	2.36	158.6
C(51)–H(51)–F(2)	3.10	2.32	138.3
C(53)–H(53)–F(4)	3.25	2.35	158.4
C(77)–H(77B)–F(1)	3.22	2.25	168.5
C(31)–H(31)–F(5)	3.15	2.24	158.5
C(41)–H(41)–F(6)	3.16	2.34	143.9
C(72)–H(72B)–F(5)	3.12	2.37	132.0
C(77)–H(77A)–F(6)	3.29	2.46	141.1

4.3. Synthesis of {p-$C_6H_4[CH_2OCH_2C(pz)_3]_2$-$[Mn(CO)_3]_2$}$(BF_4)_2$ (**1**)

A mixture of $Mn(CO)_5Br$ (0.275 g, 1.0 mmol) and $AgBF_4$ (0.194 g, 1.0 mmol) was dissolved in acetone (50 ml). The solution was heated at reflux for 1 h and the yellow solution was cannula filtered into a solution of *p*-$C_6H_4[CH_2OCH_2C(pz)_3]_2$ (0.295 g, 0.50 mmol) in acetone (50 ml). The resulting mixture was heated at reflux for 2 h and then stirred for another 2 h. Removal of the solvent yielded a yellow solid (0.374 g, 36%), melting point (m.p.) = 163 °C with decomposition. ES^+MS: Calc. for [{*p*-$C_6H_4[CH_2OCH_2C(pz)_3Mn(CO)_3]_2$}-$(BF_4)$]$^+$: 954.1136. Found: 954.1168. ^{1}H-NMR (ace-

tone-d_6, all br): δ 8.67, 8.60 (6,6H, 3,5-H pz), 7.61 (4H, C_6H_4), 6.73 (6H, 4-H pz), 5.93 (4H, $OCH_2C(pz)_3$), 5.23 (4H, OCH_2Ph). IR (Nujol) νCO: 2053, 1943 cm^{-1}.

4.4. Synthesis of $\{p\text{-}C_6H_4[CH_2OCH_2C(pz)_3]_2\text{-}[Mn(CO)_3]_2\}(OTf)_2$ (2)

This compound was prepared as above for **1** using 0.256 g of $AgCF_3SO_3$ instead of $AgBF_4$. The procedure yielded 0.382 g (66%) of **2**, m.p. = 182 °C with decomposition. Calc. for $C_{38}H_{30}F_6Mn_2N_{12}O_{14}S_2$: C, 39.12; H, 2.59. Found: C, 39.54; H, 2.31%. ^{1}H-NMR (acetone-d_6, all br.): δ 8.70, 8.63 (6,6H, 3,5-H pz), 7.65 (4H, C_6H_4), 6.70 (6H, 4-H pz), 5.90 (4H, $OCH_2C(pz)_3$), 4.98 (4H, OCH_2Ph). IR (Nujol) νCO: 2054, 1945 cm^{-1}.

4.5. Synthesis of $\{m\text{-}C_6H_4[CH_2OCH_2C(pz)_3]_2\text{-}[Mn(CO)_3]_2\}(BF_4)_2$ (3)

This compound was prepared as above for **1** using 0.295 g of m-$C_6H_4[CH_2OCH_2C(pz)_3]_2$ instead of p-$C_6H_4[CH_2OCH_2C(pz)_3]_2$. The procedure yielded 0.373 g (36%) of **3**, m.p. = 198 °C with decomposition. ES^+MS: Calc. for $[\{m\text{-}C_6H_4[CH_2OCH_2C(pz)_3Mn(CO)_3]_2\}(BF_4)]^+$: 955.1106. Found: 955.1082; ^{1}H-NMR (acetone-d_6, all br): δ 8.52, 8.47 (6,6H, 3,5-H pz), 7.77, 7.46, 7.33 (m, 4H, C_6H_4), 6.55 (6H, 4-H pz), 5.78 (4H, $OCH_2C(pz)_3$), 5.10 (4H, OCH_2Ph). IR (Nujol) νCO: 2052, 1947 cm^{-1}.

4.6. Synthesis of $\{1,2,4,5\text{-}C_6H_2[CH_2OCH_2C(pz)_3]_4\text{-}[Mn(CO)_3]_4\}(BF_4)_2$ (4)

A mixture of $Mn(CO)_5Br$ (0.22 g, 0.8 mmol) and $AgBF_4$ (0.156 g, 0.8 mmol) were dissolved in acetone (50 ml). The solution was heated at reflux for 1 h and the yellow solution was transferred via cannula over a suspension of *1,2,4,5*-$C_6H_2[CH_2OCH_2C(pz)_3]_4$ (0.22 g, 0.2 mmol) in acetone (50 ml). The resulting mixture was heated at reflux for 2 h as the ligand dissolved. After additional heating (3 h) a yellow compound precipitated that was filtered (0.256 g 62%), m.p. = 225 °C with decomposition. Calc. for $C_{66}H_{54}B_4F_{16}Mn_4N_{24}O_{16}$: C, 39.51; H, 2.71. Found: C, 39.16; H, 3.19%. ^{1}H-NMR (CD_3CN, all br): δ 8.20, 8.11 (12,12H, 3,5-H pz) 7.99 (2H, C_6H_2), 5.95 (12H, 4-H pz), 5.48 (8H, $OCH_2C(pz)_3$), 5.25 (8H, OCH_2Ph). IR (Nujol) νCO: 2051, 1943 cm^{-1}.

5. Crystallographic studies

Crystal, data collection and refinement parameters are given in Tables 1 and 2. Single crystals of **1**, **2**, **3** and **4** were grown by vapor phase diffusion of diethyl ether into an acetonitrile solution of the compounds. Suitable crystals of **1**, **3** and **4** were mounted onto thin glass fibers using inert oil for data collection at low temperature. Compound **2** was epoxied onto the tip of a glass fiber for room temperature data collection. X-ray intensity data were measured on a Bruker SMART APEX CCD-based diffractometer (Mo–K_α radiation, $\lambda = 0.71073$ Å). Raw data frames were integrated and corrected for Lorentz and polarization effects with SAINT+ [21]. Final unit cell parameters are based on the least-squares refinement of all data with $I > 5\sigma(I)$ from each data set (2501 for **1**, 7474 for **2**, 4994 for **3**, and 6214 for **4**). Analysis of identical reflections measured at the beginning and end of data collection showed negligible crystal decay during collection for each crystal. Empirical absorption corrections were applied with the program SADABS [21]. All structures were solved by a combination of direct methods and difference Fourier synthesis, and refined against F^2 using all data (SHELXTL [22]).

Compound **1** decomposes almost instantaneously upon removal from the crystallization solvent due to rapid solvent loss (vide infra). Several attempts to transfer crystals rapidly from the mother liquor to the diffractometer cold stream were made, however, the best crystal of **1** still showed visible evidence of degradation (cracking and clouding), and broader than ideal diffraction maxima. **1** crystallizes in the space group $P2_1/c$ as determined from the systematic absences in the intensity data. The $[Mn(CO)_3(C_{30}H_{30}N_{12}O_2)Mn(CO)_3]^{2+}$ cation resides on a crystallographic inversion center. After location of all atoms of the cation and anion, a region of highly diffuse electron density remained, presumably included solvent molecules. After several attempted disorder models, the SQUEEZE [23] option in the program PLATON [24] was used to account for the disordered species. SQUEEZE calculated a solvent-accessible void volume of 1221.8 $Å^3$ per cell, corresponding to 262 electrons. The contribution of these electrons was subsequently removed from the structure-factor calculations. Note that the molecular weight, calculated density and $F(000)$ value reflect known species only. Eventually, all non-hydrogen atoms were refined with anisotropic displacement parameters; hydrogen atoms were placed in geometrically idealized positions and refined as riding atoms.

Systematic absences and intensity statistics for **2** indicated the monoclinic space group $C2/c$, which was confirmed. The $[(CO)_3Mn(C_{30}H_{30}N_{12}O_2)Mn(CO)_3]^{2+}$ cation and one diethyl ether molecule of crystallization are both situated on 2-fold rotational axes. The triflate counter-ion is severely disordered, and was modeled as occupying two orientations in a 70/30 proportion, subject to several geometric restraints (SHELX DFIX and SAME). The elongated displacement parameters for the triflate indicate more severe disorder is likely present. Eventually all non-hydrogen atoms were refined with anisotropic displacement parameters; hydrogen

atoms were placed in geometrically idealized positions and refined as riding atoms.

Compound **3** crystallizes in the triclinic system. The space group $P\bar{1}$ was assumed and confirmed by successful solution and refinement of the structure. All atoms are on positions of general crystallographic symmetry, and the cation possesses no crystallographically imposed symmetry. Non-hydrogen atoms were refined with anisotropic displacement parameters; hydrogen atoms were placed in geometrically idealized positions and refined as riding atoms.

Compound **4** crystallizes in the monoclinic space group $P2_1/c$ as determined by the systematic absences in the data set. The $\{1,2,4,5\text{-}C_6H_2[CH_2OCH_2C(pz)_3]_4\text{-}[Mn(CO)_3]_4\}^{4+}$ cation is situated on an inversion center. The asymmetric unit contains one-half of the cation, two BF_4^- anions and one Et_2O and three CH_3CN solvent molecules of crystallization. All non-hydrogen atoms were refined with anisotropic displacement parameters; hydrogen atoms were placed in geometrically idealized positions and refined as riding atoms.

6. Supplementary material

Crystallographic data for the structural analysis has been deposited with the Cambridge Crystallographic Centre, CCDC # 166559 for compound **1**, CCDC # 191610 for compound **2**, CCDC # 191611 for compound **3** and CCDC # 175724 for compound **4**. Copies of this information may be obtained free of charge from The Director, CCDC, 12 Union Road, Cambridge CB2 1EZ, UK (Fax: +44-1223-336033; e-mail: deposit@ccdc.cam.ac.uk or www: http://www.ccdc.cam.ac.uk).

Acknowledgements

We thank the National Science Foundation (CHE-0110493) for support. The Bruker CCD Single Crystal Diffractometer was purchased using funds provided by the NSF Instrumentation for Materials Research Program through Grant DMR:9975623.

References

[1] (a) C. Piquet, G. Bernardinell, G. Hopfgartner, Chem. Rev. 97 (1997) 2005;
(b) P.J. Hagrman, D. Hagrman, J. Zubieta, Angew. Chem. Int. Ed. 38 (1999) 2638;
(c) A.N. Khlobystov, A.J. Blake, N.R. Champness, D.A. Lemenovskii, G. Majouga, N.V. Zyk, M. Schroder, Coord. Chem. Rev. 222 (2001) 155;
(d) A.J. Blake, N.R. Champness, P. Hubberstey, W.S. Li, M.A. Withersby, M. Schroder, Coord. Chem. Rev. 183 (1999) 117;
(e) S.T. Batten, R. Robson, Angew. Chem. Int. Ed. 37 (1998) 1461;
(f) P. Nguyen, P. Gomez-Elipe, I. Manners, Chem. Rev. 99 (1999) 1515;
(g) S. Leininger, B. Olenyuk, P.J. Stang, Chem. Rev. 100 (2000) 853;
(h) A.J. Blake, N.R. Champness, P.A. Cooke, J.E.B. Nicolson, Chem. Commun. (2000) 665;
(i) J.-M. Lehn, Chem. Eur. J. 6 (2000) 2097;
(j) D.P. Funeriu, J.-M. Lehn, K.M. Fromm, D. Fenske, Chem. Eur. J. 6 (2000) 2103.

[2] (a) I. Haiduc, T.F. Edelmann, Supramolecular Organometallic Chemistry, Wiley-VCH, 1999;
(b) D. Braga, F. Grepioni, J. Chem. Soc. Dalton Trans. (1999) 1;
(c) D. Braga, F. Grepioni, G.R. Desiraju, Chem. Rev. 98 (1998) 1375;
(d) D. Braga, F. Grepioni, Coord. Chem. Rev. 183 (1999) 19;
(e) D. Braga, L. Maini, M. Polito, L. Scaccianoce, G. Cojazzi, F. Grepioni, Coord. Chem. Rev. 216–217 (2001) 225.

[3] (a) K.A. Hirsch, S.R. Wilson, J.S. Moore, Inorg. Chem. 36 (1997) 2960;
(b) A.J. Blake, N.R. Champness, P.A. Cooke, J.E.B. Nicolson, C.J. Wilson, Chem. Soc. Dalton Trans. (2000) 3811;
(c) S.-P. Yang, X.-M. Chen, L. Ji, J. Chem. Soc. Dalton Trans. (2000) 2337;
(d) B.-L. Fei, W.-Y. Sun, K.-B. Yu, W.-X. Tang, J. Chem. Soc. Dalton Trans. (2000) 805;
(e) R.L. Paul, S.M. Couchman, J.C. Jeffery, J.A. McCleverty, Z.R. Reeves, M.D. Ward, J. Chem. Soc. Dalton Trans. (2000) 845

[4] (a) M.A. Withersby, A.J. Blake, N.R. Champness, P. Hubberstey, W.-S. Li, M. Schröder, Angew. Chem. Int. Ed. 36 (1997) 2327;
(b) R. Vilar, D.M.P. Mingos, A.J.P. White, D.J. Williams, Angew. Chem. Int. Ed. 37 (1998) 1258;
(c) M.C. Hong, W.P. Su, R. Cao, M. Fujita, J.X. Lu, Chem. Eur. J. 6 (2000) 427.

[5] (a) M.A. Withersby, A.J. Blake, N.R. Champness, P.A. Cooke, P. Hubberstey, W.-S. Li, M. Schröder, Inorg. Chem. 38 (1999) 2259;
(b) S. Subramanian, M.J. Zaworotko, Angew. Chem. Int. Ed. 34 (1995) 2127;
(c) J.T. Lu, T. Paliwala, S.C. Lim, C. Yu, T. Niu, A. Jacobson, J. Inorg. Chem. 36 (1997) 923.

[6] Strong hydrogen bonds include interactions of the type O–H···O, N–H···O, O–H···N and N–H···N. See for example: ref [2b]; (a) M.T. Allen, A.D. Burrows, M.F. Mahon, J. Chem. Soc. Dalton Trans. (1999) 215; (b) U. Ziener, E. Breuning, J.-M. Lehn, E. Wegelius, K. Rissanen, G. Baum, D. Fenske, G. Vaughan, Chem. Eur. J. 6 (2000) 4132; (c) R. Goddard, R.M. Claramunt, C. Escolastico, J. Elguero, New J. Chem. (1999) 237.

[7] Weak hydrogen bonds (X–H···Y) involve less electronegative atoms; we discuss here only C–H···Y type of weak hydrogen bond (Y = O, F). See for example: (a) M.J. Calhorda, Chem. Commun. (2000) 801; (b) G.R. Desiraju, Acc. Chem. Res. 29 (1996) 441; (c) F. Grepioni, G. Cojazzi, S.M. Draper, N. Scully, D. Braga, Organometallics 17 (1998) 296; (d) H.C. Weiss, R. Boese, H.L. Smith, M.M. Haley, Chem. Commun. (1997) 2403.

[8] C.J. Janiak, Chem. Soc. Dalton Trans. (2000) 3885 and references therein.

[9] (a) H. Takahashi, S. Tsuboyama, Y. Umezawa, K. Honda, M. Nishio, Tetrahedron 56 (2000) 6185;
(b) S. Tsuzuki, K. Honda, T. Uchimaru, M. Mikami, K. Tanabe, J. Am. Chem. Soc. 122 (2000) 11450;
(c) O. Seneque, M. Giorgi, O. Reinaud, Chem. Commun. (2001) 984;
(d) H.C. Weiss, D. Blaser, R. Boese, B.M. Doughan, M.M. Haley, Chem. Commun. (1997) 1703;
(e) N.N.L. Madhavi, A.K. Katz, H.L. Carrell, A. Nangia, G.R. Desiraju, Chem. Commun. (1997) 2249;

(f) N.N.L. Madhavi, A.K. Katz, H.L. Carrell, A. Nangia, G.R. Desiraju, Chem. Commun. (1997) 1953.
[10] (a) D.S. Reddy, D.C. Craig, G.R. Desiraju, J. Am. Chem. Soc. 118 (1996) 4090;
(b) J. Kowalik, D. VanDerveer, C. Clower, L.M. Tolbert, Chem. Commun. (1999) 2007;
(c) M. Freytag, P.G. Jones, B. Ahrens, A.K. Fischer, New J. Chem. 23 (1999) 1137;
(d) R. Thaimattam, D.S. Reddy, F. Xue, T.C.W. Mak, A. Nangia, G.R. Desiraju, New J. Chem. (1998) 143.
[11] (a) G.R. Desiraju, Angew. Chem. Int. Ed. 34 (1995) 2311;
(b) A.J. Blake, G. Baum, N.R. Champness, S.S.M. Chung, P.A. Cooke, D. Fenske, A.N. Khlobystov, D.A. Lemenovskii, W.-S. Li, M.J. Schroder, Chem. Soc. Dalton Trans. (2000) 4285;
(c) D.S. Reddy, Y.E. Ovchinnikov, O.V. Shishkin, Y.T. Struchkov, G.R. Desiraju, J. Am. Chem. Soc. 118 (1996) 4085;
(d) F.H. Allen, V.J. Hoy, J.A.K. Howard, V.R. Thalladi, G.R. Desiraju, C.C. Wilson, G.J. McIntyre, J. Am. Chem. Soc. 119 (1997) 3477;
(e) R. Thaimattam, F. Xue, J.A.R.P. Sarma, T.C.W. Mak, G.R. Desiraju, J. Am. Chem. Soc. 123 (2001) 4432;
(f) S.S. Kuduva, D.C. Craig, A. Nangia, G.R. Desiraju, J. Am. Chem. Soc. 121 (1999) 1936.
[12] (a) D.L. Reger, J.E. Collins, A.L. Rheingold, L.M. Liable-Sands, Organometallics 15 (1996) 2029;
(b) D.L. Jameson, R.K. Castellano, Inorg. Syn. 32 (1998) 51;
(c) C. Titze, J. Hermann, H. Vahrenkamp, Chem. Ber. 118 (1995) 1095;
(d) D.L. Reger, J.E. Collins, R. Layland, R.D. Adams, Inorg. Chem. 35 (1996) 1372;
(e) D.L. Reger, J.E. Collins, M.A. Matthews, A.L. Rheingold, L.M. Liable-Sands, I.A. Guzei, Inorg. Chem. 36 (1997) 6266;
(f) D.L. Reger, J.E. Collins, A.L. Rheingold, L.M. Liable-Sands, G.P.A. Yap, Inorg. Chem. 36 (1997) 345;
(g) D.L. Reger, Comments Inorg. Chem. 21 (1999) 1;
(h) D.L. Reger, C.A. Little, A.L. Rheingold, M. Lam, T. Concolino, A. Mohan, G.J. Long, Inorg. Chem. 39 (2000) 4674;
(i) D.L. Reger, C.A. Little, A.L. Rheingold, M. Lam, L.M. Liable-Sands, B.M. Rhagitan, T. Concolino, A. Mohan, G.J. Long, V. Briois, F. Grandjean, Inorg. Chem. 40 (2001) 1508;
(j) P.K. Byers, A.J. Canty, R.T. Honeyman, Adv. Organomet. Chem. 34 (1992) 1.
[13] (a) S. Trofimenko, Acc. Chem. Res. 4 (1971) 17;
(b) S. Trofimenko, J. Am. Chem. Soc. 89 (1967) 3170;
(c) S. Trofimenko, J. Am. Chem. Soc. 89 (1967) 6288;
(d) A. Shaver, J. Organomet. Chem. Lib. 3 (1976) 157;
(e) S. Trofimenko, Prog. Inorg. Chem. 34 (1988) 115;
(f) S. Trofimenko, Chem. Rev. 93 (1993) 943;
(g) S. Trofimenko, J.C. Calabrese, J.S. Thompson, Inorg. Chem. 26 (1987) 1507;
(h) S. Trofimenko, Scorpionates—The Coordination Chemistry of Poly(pyrazolyl)borate Ligands, Imperial College Press, London, 1999;
(i) A.S. Lipton, S.S. Mason, S.M. Myers, D.L. Reger, P.D. Ellis, Inorg. Chem. 35 (1996) 7111;
(j) D.L. Reger, S.M. Myers, S.S. Mason, D.J. Darensbourg, M.W. Holtcamp, J.H. Reibenspeis, A.S. Lipton, P.D. Ellis, J. Am. Chem. Soc. 117 (1995) 10998;
(k) D.L. Reger, S.M. Myers, S.S. Mason, A.L. Rheingold, B.S. Haggerty, P.D. Ellis, Inorg. Chem. 34 (1995) 4996;
(l) D.L. Reger, S.S. Mason, A.L. Rheingold, Inorg. Chim. Acta 240 (1995) 669;
(m) A.S. Lipton, S.S. Mason, D.L. Reger, P.D. Ellis, J. Am. Chem. Soc. 116 (1994) 10182.
[14] (a) D.L. Reger, J.E. Collins, D.L. Jameson, R.K. Castellano, Inorg. Syn. 32 (1998) 63;
(b) D.L. Reger, J.E. Collins, A.L. Rheingold, L.M. Liable-Sands, G.P.A. Yap, Organometallics 16 (1997) 349;
(c) D.L. Reger, J.E. Collins, S.M. Myers, A.L. Rheingold, L.M. Liable-Sands, Inorg. Chem. 35 (1996) 4904;
(d) D.L. Reger, T.C. Grattan, K.J. Brown, C.A. Little, J.J.S. Lamba, A.L. Rheingold, R.D. Sommer, J. Organomet. Chem. 607 (2000) 120;
(e) D.L. Reger, T.C. Grattan, Synthesis, in press.
[15] D.L. Reger, T.D. Wright, R.F. Semeniuc, T.C. Grattan, M.D. Smith, Inorg. Chem. 40 (2001) 6212.
[16] (a) D.L. Reger, R.F. Semeniuc, M.D. Smith, Inorg. Chem. 40 (2001) 6545;
(b) D.L. Reger, R.F. Semeniuc, M.D. Smith, Eur. J. Inorg. Chem. (2002) 543;
(c) D.L. Reger, R.F. Semeniuc, M.D. Smith, Inorg. Chem. Commun. 5 (2002) 278;
(d) D.L. Reger, K.J. Brown, M.D. Smith, J. Organomet. Chem., Xref: S0022-328X(02)02094-6.
[17] D.L. Reger, R.F. Semeniuc, M.D. Smith, J. Chem. Soc. Dalton Trans. (2002) 476.
[18] (a) A. Bondi, J. Phys. Chem. 68 (1964) 441;
(b) R.S. Rowland, R. Taylor, J. Phys. Chem. 100 (1996) 738.
[19] T. Steiner, Angew. Chem. Int. Ed. 41 (2002) 48.
[20] D.L. Reger, R.F. Semeniuc, M.D. Smith, Chem. Commun., unpublished results.
[21] SMART Version 5.619, SAINT+ Version 6.02a and SADABS. Bruker Analytical X-ray Systems, Inc., Madison, WI, USA, 1997.
[22] G.M. Sheldrick, SHELXTL Version 5.1, Bruker Analytical X-ray Systems, Inc, Madison, WI, USA, 1997.
[23] P.V.D. Sluis, A.L. Spek, Acta Crystallogr. Sect. A 46 (1990) 194.
[24] A.L. Spek, PLATON, a Multipurpose Crystallographic Tool, Utrecht University, Utrecht, The Netherlands, 1998.